

The February 6, 2023, Earthquakes in Turkey: A Model of the Rupture Surface Based on Satellite Radar Interferometry

Corresponding Member of the RAS V. O. Mikhailov^a, I. P. Babayantz^a, M. S. Volkova^{a,*}, E. P. Timoshkina^a, V. B. Smirnov^{b,a}, and Corresponding Member of the RAS S. A. Tikhotskiy^a

Received March 27, 2023; revised March 28, 2023; accepted March 28, 2023

Abstract—Two strike–slip faults, displacements along which caused the catastrophic earthquakes in Turkey on February 6, 2023, were mapped from satellite radar interferometry data. According to the satellite data, the relative displacements of the sides of the East Anatolian Fault Zone (EAFZ), with which the first event of M_w 7.8 was associated, exceeded 5 m in the central segment. The rupture surface extends from the area of the Doğanyol-Sivris earthquake M_w 6.7 of January 24, 2020, in the north to the Mediterranean coast in the south, where the earthquake M_w 6.3 occurred on February 20, 2023. The second event M_w 7.5 is associated with the Surgü-Çardak fault; the relative displacements of its sides, according to satellite data, exceeded 7 m. The obtained displacement fields of the Earth’s surface were used to construct a model of the seismic rupture. This model was worked out on the basis of the Pollitz, 1996 solution, which defines displacements on the surface of the spherically stratified planet as a result of along dip and strike displacements on a rectangular rupture located inside the sphere. Ignoring the spherical stratification of the planet leads to errors of up to 20%, especially in the presence of a large strike–slip component [5]. Ignoring sphericity also causes an error, when using the solution obtained for an elastic homogeneous half-space, as the US Geological Survey (USGS) has done, in modeling the seismic rupture for earthquakes in Turkey in 2023. Our model differs in the detailed consideration of the fault geometry. For this purpose, the faults were approximated by 19 planes along the strike, divided into two levels along the dip. In our rupture model strike–slip displacements in the central segment of the EAFZ reached 12.7 m. In the southern segment of this rupture, the displacements are much smaller. It should be emphasized that we registered the displacements for the period from January 29, 2023, to February 10, 2023; therefore, together with co-seismic ones, they also include post-seismic displacements for four days after the main seismic events. The displacements on the rupture surface along the Surgü-Çardak Fault, where the M_w 7.5 earthquake occurred, were up to 10 m. The results demonstrate, in particular, the efficiency of application of the satellite radar interferometry in the operative study of catastrophic geodynamic phenomena and processes.

Keywords: earthquakes of February 6, 2023, Turkey, Synthetic Aperture Radar (SAR) Interferometry, seismic rupture surface

DOI: 10.1134/S1028334X23600627

INTRODUCTION

On February 6, 2023, a series of catastrophic earthquakes occurred in southern Turkey near the border with Syria. The first earthquake of M_w 7.8 (U.S. Geological Survey (USGS) data¹) was recorded at 01:17:34 (UTC). The coordinates of the hypocenter were determined as 37.225 N, 37.021 E, 35 km to the west of the city of Gaziantep (at the border of Kahramanmaraş

Province) at a depth of 17.5 km. The epicenter is located on a small fault (the red star in Fig. 1, the position of faults is given from the database [1]), which extends to the southwest from the East Anatolian Fault Zone (EAFZ). According to the USGS, the rupture surface reached the EAFZ and moved to the northeast and southwest over more than 100 km in both directions. After nine hours, at 10:24:49 (UTC), a second big earthquake of M_w 7.5 occurred on the fault called Surgü-Çardak [2] with the epicenter at 38.024 N, 37.203 E in the area of Ekinözü settlement (Ekinözü, Kahramanmaraş Province), approximately 90 km to the north of the first event (the yellow star in Fig. 1). The hypocenter of the second event was determined to be at the depth of 13.5 km. The data on the magnitude and coordinates of hypocenters of different seismological centers differ slightly. For instance, the GCMT

¹ <https://earthquake.usgs.gov/earthquakes/>.

^aSchmidt Institute of Physics of the Earth, Russian Academy of Sciences, Moscow, 123995 Russia

^bMoscow State University, Physics Department, Moscow, 119991 Russia

*e-mail: msvolkova6177@gmail.com

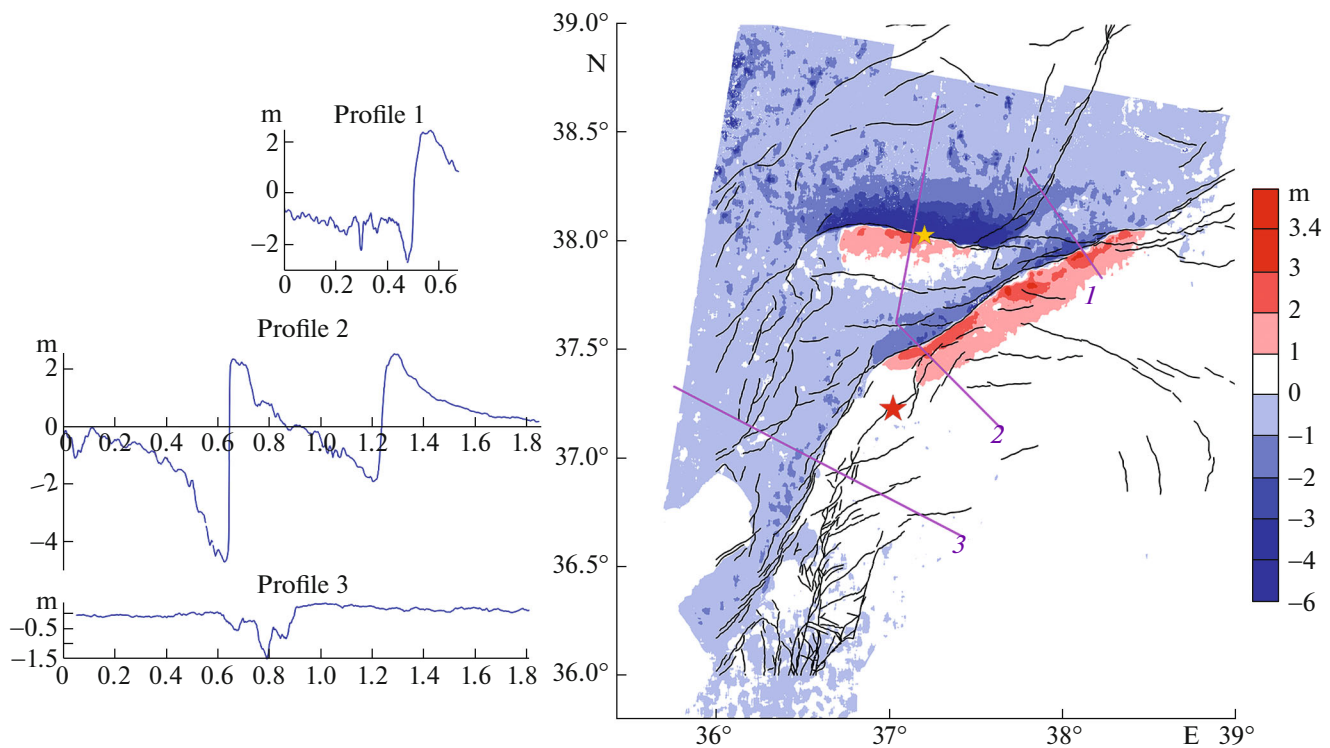


Fig. 1. The field of displacements in the direction perpendicular to the orbit (orbital azimuth 189°). Displacements are represented in meters, positive in the easterly direction. The faults were plotted using the database of active faults [1]. According to [2], the Sürgü-Çardak Fault has a northward dip and the EAFZ dips to north-west with an angle of 80° . The displacements along the profiles, marked with numbers 1–3, are shown on the left, where the horizontal axis shows the distance in map units. The profile number on the map corresponds to its right end in the profile on the left.

(Global Centroid Moment Tensor²) estimates the magnitudes of the earthquakes as M_w 7.8 and 7.7 with the epicenters at (37.56 N, 37.47 E) and (38.11 N, 37.22 E). These earthquakes and their numerous aftershocks located in the zone of East Anatolian Fault covered 11 provinces of the region with a total area of 108 812 km² and became the most destructive in the history of the country (data of the Ministry of Emergencies of the Turkish Republic—AFAD³). The earthquakes caused surface ruptures and fractures, with predominating left-lateral strike-slip displacements. According to the AFAD data, the total length of surface ruptures of the first earthquake was 290 km, the maximum strike-slip displacements reached 5.5 m at the area west of Çiğli¹ to the settlement of Türkoğlu. The rupture, as a result of the second earthquake, extended for 130 km. In the area north of Gölbaşı to the settlement of Barysh, the maximum displacement was up to 6 m. Subsequently, rockslides, landslides, and soil liquefaction were also observed. The event of February 6, 2023, is recognized as one of the most catastrophic since the beginning of the 21st century because of the large-scale catastrophic destruction of residential buildings and con-

structions. It ranks fifth in the number of human casualties. According to USGS, the number of dead and injured exceeded 160 000; 1.5 million people were left homeless, and more than 164 000 buildings were destroyed.

In terms of tectonics, the EAFZ is the boundary between the Anatolian and Arabian plates. The rate of relative displacement of the Arabian Plate ranges from 6 mm/year in the southern part to 10 mm/year in the northern part of the East Anatolian Fault Zone.

Due to the enormous destruction and loss, detailed geological study of such an extended focal zone will not be possible very soon. Under these conditions, various satellite data, including satellite radar interferometry, are of significant help.

METHODS AND RESULTS

Satellite synthetic aperture radars (SAR) make it possible to imaging the Earth's surface regardless of weather and illumination with a spatial resolution of a few meters. The images from the Sentinel-1A satellite used in this work, have dimensions of 200×250 km². Joint processing of a pair of images of the same territory makes it possible to determine the displacements of the reflecting objects on the Earth's surface during

² <https://www.globalcmt.org/CMTsearch.html>.

³ <https://deprem.afad.gov.tr/home-page>.

the time between repeated imaging. The radar image contains information about the amplitude and the phase of the radar signal reflected from a resolution element on the Earth's surface. The analysis of the phase difference of radar signals, received during repeated imaging of the same object, allows us to determine its displacement in the direction of radar signal propagation, i.e., in the direction to the satellite. Due to the fact that the changes of phases are registered in range from $-\pi$ to π , it is necessary to reconstruct the full phase of the reflected signal. This operation is called phase unwrapping and consists in adding the necessary number of full periods to the recorded phase. The phase unwrapping is an ambiguous operation, so it is conducted under the condition that the phase must not change by more than half a period in neighboring elements of resolution. For this reason, it is difficult to unwrap the phase in the areas of large displacements, in particular near the seismic rupture, where the displacements may be meters or more. This method gives an accuracy of the displacement estimation of a few centimeters [3].

There is also the method of offsets, which is applied in cases of large displacements. It consists in identifying the same elements of resolution in the field of the amplitude of the reflected signal. The offsets by this method are estimated at the subpixel level, with a pixel size of a few meters. The accuracy of this method is lower than that of the reflected signal phase analysis, but it allows us to carry out estimations consistently in the areas where displacements reach several meters or more. The offset method allows us to estimate displacements perpendicular to the orbit (in the range) and parallel to the orbit (in the azimuth of flight of the satellite). These offsets are close to the northward and eastward offsets, because the orbit of the Sentinel-1A satellite deviates from the north-south direction by not more than ten degrees.

To estimate the displacements, we used SAR images from Sentinel-1A taken from the ascending and descending orbits before and after February 6, 2023. The most distinct picture is obtained in the displacements in the range from the descending orbit with the azimuth of 189° on the basis of the images from January 29 and February 10, 2023 (Fig. 1).

Let us denote the angle between the strike of the fault and the orbit of the satellite by β . Then the displacements of the reflecting object perpendicular to the descending orbit (R), along its azimuth (Az), and in the direction to the satellite (U_{los}) (positive to the east, north, and to the satellite), will be equal:

$$\begin{aligned} R &= U_{ss} \sin(\beta), & Az &= U_{ss} \cos(\beta), \\ U_{\text{los}} &= U_{\text{up}} \cos(\theta) + R \sin(\theta). \end{aligned} \quad (1)$$

Here, U_{ss} is the amplitude of strike-slip displacements and U_{up} is the amplitude of vertical displacements on the fault sides; θ is the incidence angle of the radar emission.

The relative displacements of the Sürgü-Çardak Fault sides extend up to 7 m in the range. They are close to the amplitude of strike-slip displacements on the fault, because the fault strike is almost perpendicular to the descending orbit, i.e., β is close to 90° . The displacements in the range at the EAFZ are smaller than the strike-slip displacements on the fault, because β varies from 10° to 70° for different fault segments. In the area of profile 2 (Fig. 1), the range displacements on the EAFZ exceeded 4 m. Taking into account the angle between the satellite's orbit and the fault strike, which is 53° in this area, the relative displacement of the sides here exceeded 5 m (Eq. (1)).

Displacements in the direction of satellite flight from the ascending and descending orbits, as well as the displacements in the range from the images from the ascending orbit, were also obtained. The maps of these offsets match well. They will be analyzed in a more detailed publication. Figure 2 shows the displacements toward the satellite U_{los} (Eq. (1)) obtained from a pair of the same images.

In general, the maps of displacements agree well with each other (taking into account the fact that the amplitude of the displacements to the satellite, according to Eq. (1) in the absence of the vertical component U_{up} differs from the displacements in the range in $\sin(\theta) \approx \sin(38^\circ) = 0.615$ times). This indicates a significant predomination of the strike-slip component over the vertical displacements. The only significant divergence is observed on the EAFZ in the area of profile 5 in Fig. 2, where the area of positive displacements in the satellite direction is located on both sides of the EAFZ, whereas on the map of displacements in the range (Fig. 1), the displacements change sign when crossing the EAFZ. The Gölbaşı sedimentary basin is located in this area [4]. The discrepancy may be due to the presence of the vertical component U_{up} , which is included in the displacements toward the satellite, but is not included in the displacements in the range. It should also be taken into account that the coherence in this area is low due to the steep mountainous relief and because of the presence of several large water bodies. This could lead to errors in the phase unwrapping. The divergence of the maps of displacements in this area requires detailed study.

Let us note the displacements along profile 4 in Fig. 2, which crosses the fault, where the seismic rupture began and along which the deformation propagated to EAFZ. The displacements here are relatively small, and contain strike-slip and possibly thrust component.

MODEL OF THE RUPTURE SURFACE

The field of displacements in the range was used to plot a model of the rupture surface. For this purpose, the Sürgü-Çardak Fault was divided into four elements along its strike, and the EAFZ was divided into

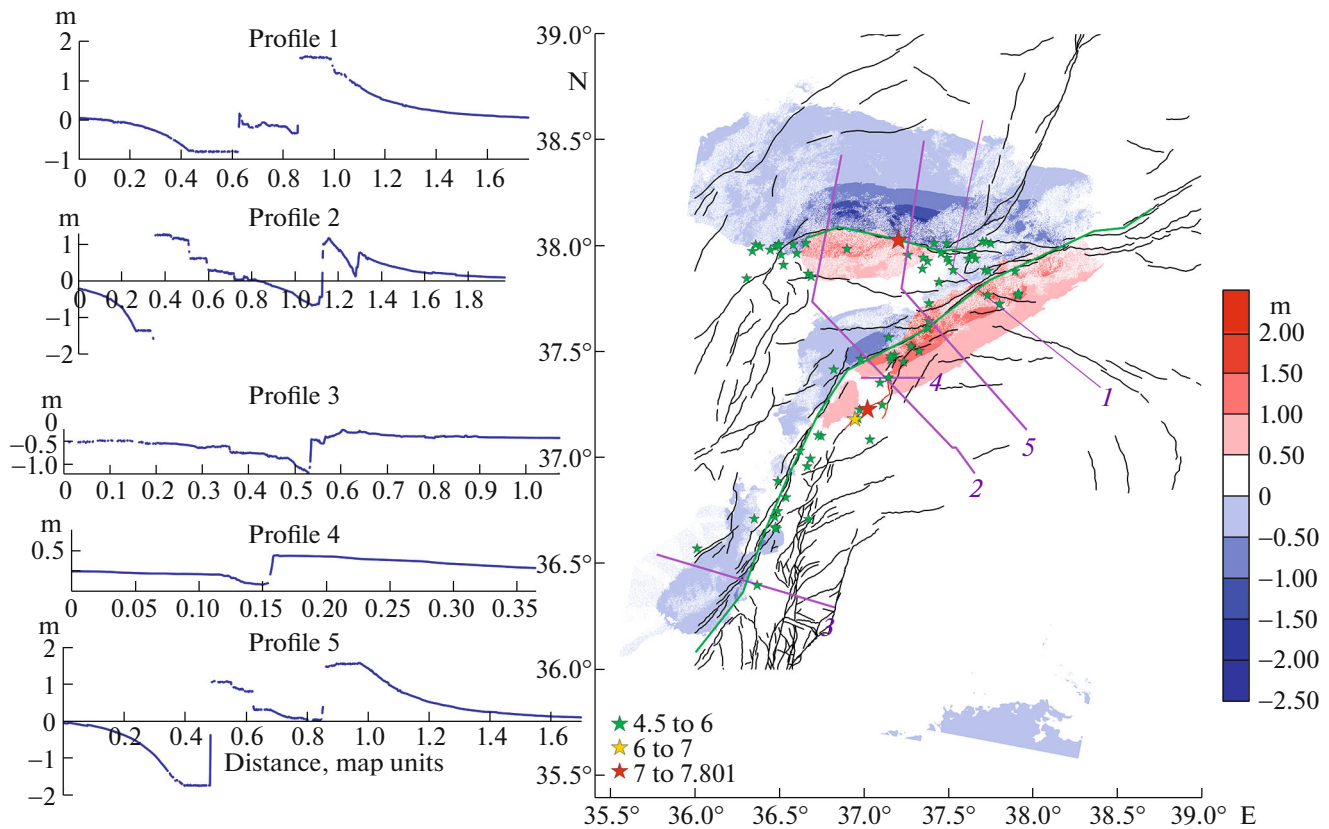


Fig. 2. The displacements (in meters) calculated using the paired interferogram of the Sentinel-1A satellite images from the descending orbit on January 29 and February 10, 2023. The green line is the boundary between the negative and positive displacements obtained by the offset method (Fig. 1). The plots of displacements along the profiles, marked by numbers, are shown on the left. Stars are the epicenters of the strongest earthquakes and aftershocks with magnitude more than 4 for the period between radar images.

15 elements (Fig. 3), including seven elements in its southern part with a south-southwesterly strike, and eight elements in its northern part with a west-southwesterly strike. The rupture on the Sürgü-Çardak Fault was given from a depth of 0.5 to 20 km with a dip northward at an angle of 80° . At EAZF, the depth of the upper edge was given as 1 km; the lower edge was given as 20 km with a dip northwestward at an angle of 85° according to [1, 2]. The small rupture from which the earthquakes began was not included in the model at this stage. In terms of depth, the models are divided into two levels of equal length along the dip. The solution was found under the condition that the displacements were close to pure strike-slip. We used a model of displacements on the surface of a spherically stratified planet as a result of a slip along the dip and strike on a rectangular cut located at a given depth [5]. The methodology for solving this problem is described in detail in [7].

In the model of the rupture surface shown in Fig. 3, arrows indicate the directions of displacements on a hanging wall of the fault. For the EAFZ, a dip was given to the northwest at an angle of 85° ; however, the results change little if the dip is given to south-east at

the same angle. It should be noted that the seismological data (USGS) indicate that the focal plane parallel to the EAFZ dips to the southeast, but the geological data [1, 2] indicate that it dips to the northwest.

In the southern segment of the EAFZ, the displacements increase monotonically from south to north. The displacements in the upper part of the rupture are greater than in the lower part, except for the southernmost element, in the lower part of which the displacements were 3.5 m, and in the upper part, less than 0.5 m. This is where the earthquake of M_w 6.3 with the hypocenter located at a depth of 11.5 km occurred on February 20, 2023, after the period covered by the SAR images.

Further northward, the amplitude of the displacements in the upper part of the southern segment of the seismic rupture increased to 5.6 m; in the lower part of the rupture, their maximum did not exceed 3.4 m.

In the central segment of the EAFZ, where its strike turns to west-southwesterly, the displacement amplitude at the seismic rupture increases significantly. The displacements in the upper part of the rupture in some places exceeded 8 m, and in the lower

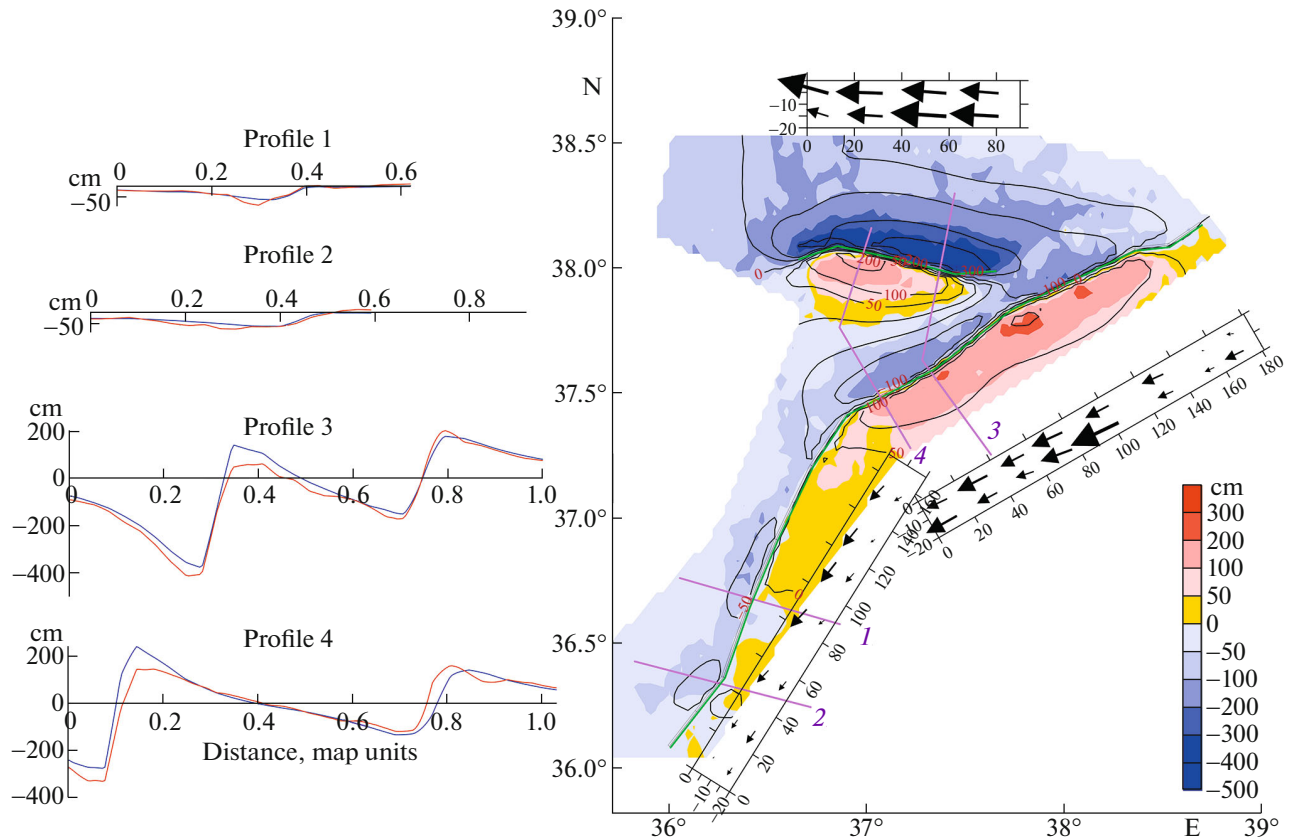


Fig. 3. The model of the rupture surface of the February 6, 2023, earthquake based on the SAR interferometry data. The color map shows the displacements of the Earth's surface (cm), determined by the offset method from the images of the descending orbit. Black isolines are the displacements of the Earth's surface calculated from the model. Black rectangles show the rupture surface in the vertical section, with the displacements at the upper and lower levels. The maximum length of an arrow is 12.7 m in the middle part of the northern segment of the EAFZ. Dark red lines are profiles through the rupture area. The SAR data (red) and model fit (blue) for these profiles are shown on the left.

part, on one of the elements, the displacements were up to 12.7 m. Further northward, the displacements decreased, but still at the lower level of the northernmost segment, they were up to 5 m. This area reaches the seismic rupture of the Doğanyol-Sivrice earthquake M_w 6.7 January 24, 2020, according to the model of this event published on the USGS website.

The distinct strike-slip displacements occurred on three eastern segments of the rupture along the Sürgü-Çardak Fault, and on its western segment, where the rupture turns southward, a thrust component is added (Fig. 4). The displacements in the upper part of the rupture increase from east to west. In the lower part of the rupture, more intense displacements occurred in the eastern part.

DISCUSSION AND CONCLUSIONS

The SAR interferometry data allowed us to map two strike-slip faults, displacements on which caused the earthquakes of magnitude 7.8 and 7.5. The first event is attributed to the East Anatolian Fault Zone. The relative displacements in range in the area of profile 2 (Fig. 1) exceeded 6 m according to the satellite

data. The rupture surface extends from the area of the Doğanyol-Sivrice earthquake of M_w 6.7 on January 24, 2020, in the north to the Mediterranean Sea coast in the south, where the earthquake of M_w 6.3 occurred on February 20, 2023. The maximum relative displacements of the sides of the Sürgü-Çardak Fault according to the SAR-data were estimated at 7 m.

Data on displacements of the Earth's surface were used to construct the model of the seismic rupture surface. The model was worked out on the basis of the solution in [5], where formulas were obtained for calculating the displacements on the surface of the spherically layered planet as a result of displacements along dip and strike on a rectangular cut located inside the sphere. It is important that ignoring the spherical layering of the planet, according to [5], leads to errors up to 20%. The largest errors occur in the presence of a large strike-slip component. Ignoring sphericity also introduces an error when using a solution within idealization of the elastic homogeneous half-space [6], as the USGS did in design the seismic rupture models for the earthquakes in Turkey in 2023.

The difference between our model and the USGS one is in the more detailed geometry of the seismic

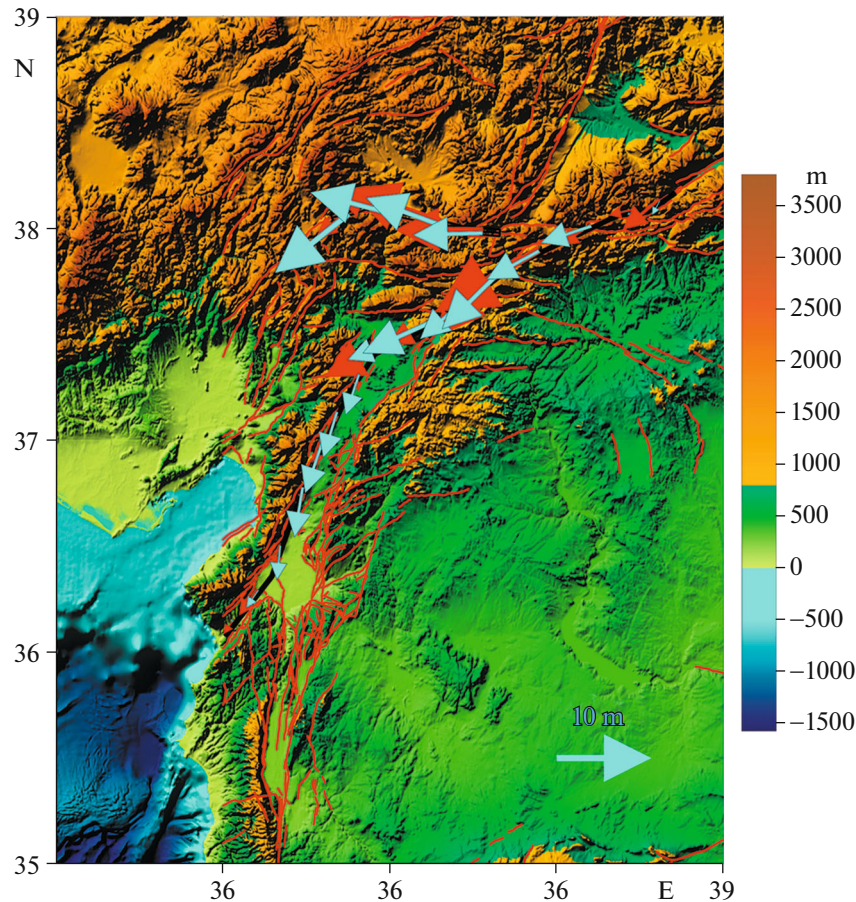


Fig. 4. Model of the rupture surface of the February 6, 2023, earthquake on the topographic map based on data from the website of the US National Center for Environmental Information.⁴ The black line is the projection of the planes approximating the rupture surface to the day surface; red lines are the faults in the database [1]. Blue arrows are displacements in the upper level; red arrows are displacements in the lower level.

rupture surface. For this purpose, we approximated the rupture by 19 planes along the strike, divided into two levels along the dip. According to our model, strike-slip displacements on the central segment of the seismic rupture along the EAFZ reached 12.7 m. In the southern segment of this rupture, the displacements are considerably smaller. It should be emphasized that we recorded the surface displacements of the Earth's surface for the period January 29, 2023, to February 10, 2023. Therefore, they include also post-seismic displacements for four days after the main seismic events.

The rupture surface model, published on the USGS website, similarly to our model, shows that the displacements increase from south to north at the southern end of the EAFZ and are generally concentrated in the upper part of the seismic rupture to a depth of 12–14 km. At the southern end of this rupture, the displacements in our model are slightly

larger. The USGS model also has an area of intense displacement at the top of the central segment of the rupture along the EAFZ. The displacements in both models go deep in the area in which we have obtained displacements greater than 12 m, although the amplitude of the displacements in the USGS model does not exceed 5 m here.

In the USGS model on the Sürgü-Çardak Fault, the seismic rupture, just as in our model, goes down to a depth of 20 km, and the displacement amplitude extends up to 12 m.

The results once again show the efficiency of application of satellite radar interferometry in studying geodynamic processes.

FUNDING

This work was carried out according to a State Assignment of the Schmidt Institute of Physics of the Earth, Russian Academy of Sciences.

⁴ <https://www.ngdc.noaa.gov/>.

CONFLICT OF INTEREST

The authors declare that they have no conflicts of interest.

OPEN ACCESS

This article is licensed under a Creative Commons Attribution 4.0 International License, which permits use, sharing, adaptation, distribution and reproduction in any medium or format, as long as you give appropriate credit to the original author(s) and the source, provide a link to the Creative Commons license, and indicate if changes were made. The images or other third party material in this article are included in the article's Creative Commons license, unless indicated otherwise in a credit line to the material. If material is not included in the article's Creative Commons license and your intended use is not permitted by statutory regulation or exceeds the permitted use, you will need to obtain permission directly from the copyright holder. To view a copy of this license, visit <http://creativecommons.org/licenses/by/4.0/>.

REFERENCES

1. D. M. Bachmanov, A. I. Kozhurin, and V. G. Trifonov, *Geodynam. Tectonophys.* **8** (4), 711–736 (2017).
2. R. Basili et al., *The European Database of Seismogenic Faults (EDSF) Compiled in the Framework of the Project SHARE* (2013).
<https://doi.org/10.6092/INGV.IT-SHARE-EDSF>
3. A. Ferretti, *Satellite InSAR Data: Reservoir Monitoring from Space (EET 9)* (Earthdoc, 2014).
4. R. O. B. Westaway and J. A. N. Arger, *J. Geol. Soc.* **153** (5), 729–744 (1996).
5. F. F. Pollitz, *Geophys. J. Int.* **125** (1), 1–14 (1996).
6. Y. Okada, *Bull. Seismol. Soc. Am.* **75** (4), 1135–1154 (1985).
7. V. O. Mikhailov, A. N. Nazaryan, V. B. Smirnov, M. Diament, N. M. Shapiro, E. A. Kiseleva, S. A. Tikhotskii, S. A. Polyakov, E. I. Smol'yaninova, and E. P. Timoshkina, *Izv., Phys. Solid Earth* **46** (2), 91–104 (2010).

Translated by V. Krutikova

Publisher's Note. Pleiades Publishing remains neutral with regard to jurisdictional claims in published maps and institutional affiliations.